Reflection Contrast Microscopy for High Resolution Detection of ^{3}H-Estradiol in Ultrathin Sections of Human Stratum Corneum

JAN A. M. NEELISSEN,[1]* AD H. G. J. SCHRIJVERS,[2] HANS E. JUNGINGER,[3] AND HARRY E. BODDÉ[3]
[1]*AstraZeneca R&D Södertälje, Pharmacokinetcs and Biopharmaceutics, 151 85 Södertälje, Sweden*
[2]*Laboratory for Electron Microscopy, Leiden University, 2333 AA Leiden, The Netherlands*
[3]*Leiden/Amsterdam Center for Drug Research, Pharmaceutical Technology, 2300 RA Leiden, The Netherlands*

KEY WORDS cryo-fixation; freeze-drying; autoradiography

ABSTRACT A single autoradiographical method for light and electron microscopy (LM and EM) is presented. Human skin, containing ^{3}H-estradiol (^{3}H-E2) after an in vitro permeation experiment, was processed via a non-extractive tissue preparation protocol, comprising cryo-fixation, freeze-drying, osmium tetroxide vapor fixation, and Spurr resin embedding. Semithin sections were processed for LM autoradiography, while ultrathin sections were processed both for high-resolution LM and EM autoradiography. The autoradiographs were visualized by bright-field microscopy (BFM), reflection contrast microscopy (RCM), and transmission electron microscopy to evaluate the potentials of RCM visualization in high-resolution LM autoradiography. RCM visualization of ultrathin vs. semithin resin sections showed an improved stratum corneum morphology. Histological staining was superfluous. The localization of ^{3}H-E2 in human stratum corneum using high-resolution LM autoradiography and RCM was as accurate as with high-resolution EM autoradiography. *Microsc. Res. Tech. 47:286–290, 1999.*

Introduction

In the majority of research on localization studies in skin after topical application of a substance, LM autoradiography has been used (e.g., Bidmon et al., 1990; Conte et al., 1992; Rutherford and Black, 1969; Suzuki et al., 1978; Touitou et al., 1988; Zelei et al., 1990). Autoradiographs have been visualized with BFM (Bidmon et al., 1990; Rutherford and Black, 1969; Suzuki et al., 1978; Touitou et al., 1988) and dark-field illumination (Conte et al., 1992; Zelei et al., 1990). However, both types of illumination have some restrictions (Priestley, 1992). When using BFM, silver grains are only visible with high magnification objectives (×40–100), making analysis of large areas time-consuming and difficult. Furthermore, silver grains are often barely visible when histological stains were used. In addition, due to the narrow depth of focus of these objectives, tissue and silver grains appear in separate focal planes. As a result, either out-of-focus or multiple-exposure microphotographs have to be made (Singh, 1986). Dark-field microscopy (DFM), introduced to autoradiography by Rogers (1967), overcomes these problems. It permits a more sensitive detection and, therefore, the visualization of smaller silver grains at even lower objective magnifications (×10). However, DFM also has disadvantages. When tissue itself diffracts the light, silver grains can be obscured, a problem especially prominent when stratum corneum is studied (Conte et al., 1992). Hence, tissue and silver grains cannot be simultaneously visualized by DFM. Results often have to be presented by pairs of bright- and dark-field photomicrographs (e.g., Conte et al., 1992; Zelei et al., 1990).

When in 1983 epi-polarization microscopy (EPM) was introduced for visualization of colloidal gold probes in LM immunocytochemistry (de Mey, 1983), it barely found its way to LM autoradiography. Like DFM, EPM gives a dark-field image; however, it has some distinct advantages. When dark-field illumination is difficult, as with darkly counterstained sections (Priestley, 1992) or darkly pigmented tissue (Rapaport et al., 1992), EPM still gives very clear images of the silver grains. Additionally, EPM allows a rapid and easy switching between bright-field and epi-polarized images, or simultaneous viewing of both images (Priestley, 1992; Rapaport et al., 1992). While many people consider epi-polarization illumination the best for light microscopical observation of silver-enhanced colloidal gold and autoradiographical silver grains, there is another type of illumination suitable: reflection contrast microscopy (RCM). Although already introduced to cell biology by Ploem in 1975 (Ploem, 1975), its use to visualize heavy metal labels only appeared in 1986, when Hoefsmit et al. (1986) applied it for silver-enhanced colloidal-gold labels. Cornelese-ten Velde et al. (1990) compared RCM with EPM, and found that RCM was superior in terms of sensitivity in detecting reflecting objects, in the visualization of unstained structures and with respect to the spatial resolution. The fact that RCM of immunolabeled ultrathin sections was found to decrease the gap between LM and EM (Cornelese-ten Velde and Prins, 1990; Prins et al., 1993), led us to explore if RCM visualization of autoradiographs derived from ultrathin sections could be an alternative to high-resolution EM autoradiography. We had previously used the latter technique to localize ^{3}H-E2 in human stratum corneum after topical application in vitro (Neelissen et al., 1996, 1998).

Contract grant sponsor: Schwarz Pharma AG, Monheim, Germany.

*Correspondence to: Dr. J.A.M. Neelissen, Pharmacokinetics & Biopharmaceutics, AstraZeneca R&D Södertälje, S-151 85 Södertälje, Sweden.
E-mail: jan.neelissen@astrazeneca.com

Accepted in revised form 11 August 1999.

MATERIALS AND METHODS

Chemicals

[2,4,6,7-^{3}H]Estradiol (SA 14.6 GBq/mg) was purchased from Amersham (Buckinghamshire, UK); Freon 22 from Hoek Loos (Schiedam, The Netherlands); Osmium tetroxide from Agar Scientific LTD. (Stansted, UK); Ria Luma from Lumac LSC (Groningen, The Netherlands); Spurr resin from Bio-Rad/Polaron (Cambridge, MA); 4% Collodion in diethyl ether from Merck (Darmstadt, Germany); and Ilford L4 from Ilford Limited (Mobberley, Cheshire, England). All other chemicals used were of analytical grade. All solutions were prepared with purified water (Milli-Q UF Plus Water System, Millipore, Etten-Leur, The Netherlands). Phosphate-buffered saline (PBS) had the following composition: sodium chloride (NaCl) 8 g/l, potassium chloride (KCl) 0.19 g/l, disodium phosphate ($Na_2HPO_4 \cdot 12H_2O$) 2.86 g/l, potassium hydrogenphosphate (KH_2PO_4) 0.20 g/l, pH was set to 7.4 with 0.1 N sodium hydroxide (NaOH).

Skin

Fresh human abdominal skin was obtained from a female donor after cosmetic surgery. Following prior removal of the subcutaneous fat, the skin was dermatomed at 250 μm (Padgett Electro Dermatome model B, Kansas City, MO). The dermal side of the skin was spread on parafilm, and disks with a diameter of 16 mm were punched and stored at 4°C in a petri dish on filter paper soaked with PBS. The skin was used the next day for permeation experiments.

Preparation of the ^{3}H-E2 Patch

An estradiol (E2) containing adhesive solution for the preparation of the patch was provided by Schwarz Pharma AG (Monheim, Germany). Patches were made using Erichsen equipment (model 509/1, knife model 411/220, Hemer-Sundwig, Germany). The drug containing matrix with a thickness of 24 ± 1 μm in the dry state contained 2.49% (w/w) E2.

Permeation Experiment

Four Franz-type permeation cells with a diffusion area of 0.79 cm^2 and a receiver chamber volume of 4.4 ml, were kept at 32°C (Haake, model E52, Berlin, Germany). Two radioactive and two non-radioactive patches were applied to the stratum corneum side of the skin and mounted in the permeation cells, which had stationary degassed PBS as the receiver solution. Permeation was terminated after 8 hours.

Sample Preparation

Following permeation and careful removal of the patches, the skin samples were cut into small pieces, immediately plunged in liquid nitrogen cooled Freon 22, and stored in liquid nitrogen. The skin pieces were freeze-dried and resin embedded as described in Neelissen et al. (1996,1998). Briefly, three frozen skin pieces from each permeation cell were freeze-dried for 16 hours at −80°C and a vacuum better than $<10^{-4}$ Pa. The sample holder was heated slowly (10°C/15 minutes) to 0°C, allowed to reach room temperature overnight (22 hours), closed with a lid while still under vacuum, and moved to a desiccator. After evacuation of the desiccator (about 1 Pa), the sample holder lid was removed and the skin pieces were exposed to the vapor of solid osmium tetroxide for 3 hours. Residual osmium tetroxide vapor was removed and freshly prepared complete Spurr medium was dropped on the skin pieces while flushing them with dried nitrogen gas. Following a 30-minute infiltration under vacuum, the resin was replaced twice for a 30-minute infiltration at ambient conditions. The skin pieces were transferred to an embedding mold for polymerization at 60°C for 48 hours.

Autoradiography

Both LM and EM autoradiography were performed according to the "flat substrate" procedure as described by Salpeter (1981). Semithin (1 μm) and ultrathin sections (100 nm) were cut perpendicularly to the skin surface with a diamond knife, picked up and placed on glass slides (1 μm and 100 nm sections) or collodion coated glass slides (100 nm sections). Sections from skin pieces from all four permeation cells were placed on the same slide to ensure exactly the same autoradiographical conditions. A thin carbon layer was evaporated on the surface of the sections to prevent interactions with the photographic emulsion (positive chemography and extraction of ^{3}H-E2). Slides were dipped in a solution of Ilford L4 in water (1 μm sections in 1:1 v/v, 100 nm sections in 1:2.5 v/v) at 32°C and withdrawn at a speed of 84 mm/min (Ginsel et al., 1979; Vrensen, 1970). Slides were dried vertically at ambient conditions for 1 hour, then placed in black slide boxes containing silica gel and stored at 4°C up to 12 months. The development schedule followed was: 2 min Kodak D19b developer (Kopriwa et al., 1984), 15-second water rinse, 30-second 1% acetic acid stop, 15-second water rinse, 2-minute non-hardening fixer, and 3 × 10 minute rinse in water (all solutions were 20°C). The fixer was made fresh and contained 20% sodium thiosulfate ($Na_2S_2O_3 \cdot 5H_2O$) and 2.5% potassium metabisulfite ($K_2S_2O_5$) in water (Salpeter, 1981). Additionally, some slides were developed in the fine grain developer Gold-Elon Ascorbic acid (GEA, gold latensification 5 min, elon ascorbic acid 5 min; Salpeter, 1981). Some slides, containing either 1 μm or 100 nm sections, were counterstained with toluidine blue according to Krum et al. (1991). Ultrathin sections with the accompanying films were floated on water, covered with copper grids, and picked up with parafilm.

Examination of the Preparations

Both 1 μm and 100 nm sections, stained and unstained, were examined with a Leitz Orthoplan microscope (Leitz, Wetzlar, Germany) equipped for bright-field and reflection contrast microscopy. The reflection contrast objectives used were a Leitz NPL Fluotar 100/1.32 Oel Phaco 2 RK and a Leitz NPL Fluotar 50/1.00 Oel Phaco 2 RK (for more details on RCM see Cornelese-ten Velde and Prins, 1990). The sections were observed with immersion oil between objective and slide, while no coverslips were used. Ultrathin sections on grids were examined in a JEOL JEM-100S transmission electron microscope operating at an accelerating voltage of 60 kV.

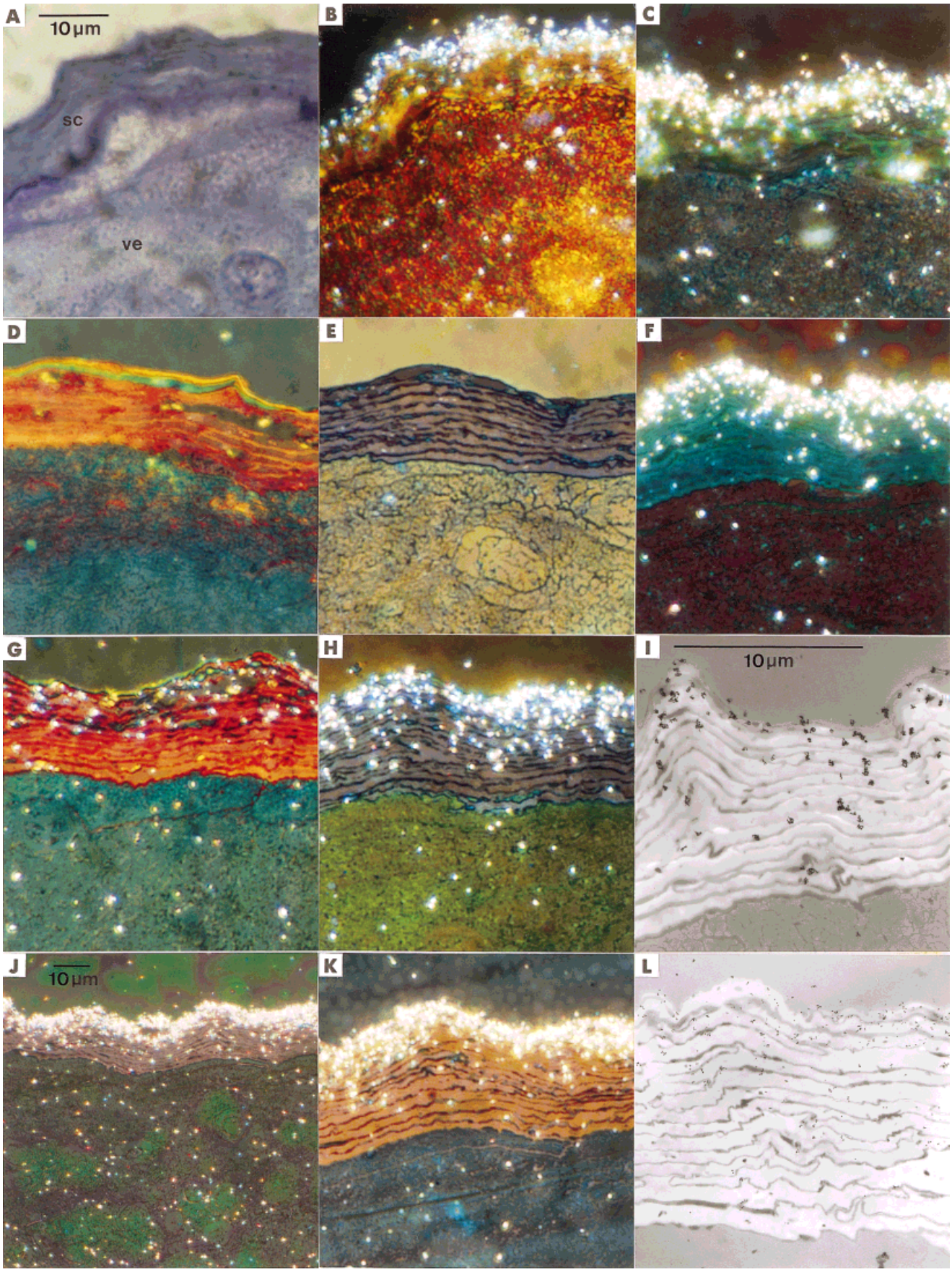

Fig. 1.

RESULTS

Semithin Sections

When toluidine blue–stained semithin sections of human stratum corneum were observed with bright-field illumination, silver grains were hard to detect due to the intense toluidine blue staining of the stratum corneum (Fig. 1 A). However, when switched to reflection contrast illumination, the grains became easily detectable as very bright dots (Fig. 1 B). Most of the grains resided over the stratum corneum, in which separate corneocytes were hard to detect. Note that the stratum corneum only partly adhered to the glass slide, because it had curled up after sectioning.

In unstained semithin sections bright-field illumination only revealed silver grains, whereas reflection contrast illumination revealed both silver grains and tissue (Fig. 1 C). Again, corneocytes were barely distinguishable in the stratum corneum, making semithin sections unfavorable for (sub)cellular localization studies.

Ultrathin Sections

Morphology. Ultrathin sections revealed a well-preserved stratum corneum morphology, with clearly distinguishable corneocytes surrounded by a well-defined intercellular domain (Fig. 1 D–L). Toluidine blue–stained ultrathin skin sections, barely visible with bright-field illumination, appeared in RCM with an orange-colored stratum corneum (Fig. 1 D). Non-stained ultrathin skin sections, invisible with bright-field illumination, appeared with brown corneocytes surrounded by a dark intercellular domain (Fig. 1 E, collodion coated slide). Both Figure 1 D and E were control autoradiographs, i.e., from permeation experiments with non-radioactive E2.

High-Resolution LM and EM Autoradiography. After Kodak D19b development, the brightly reflecting silver grains were well discernible with RCM (Fig. 1 F–H). Compared to non-stained (Fig. 1 F) and toluidine blue–stained sections (Fig. 1 G), non-stained sections on collodion coated slides resulted in the best autoradiographs with respect to stratum corneum contrast and localization of the silver grains (Fig. 1 H). Silver grains predominantly covered the superficial corneocytes, and rapidly decreased in number towards the basal corneocytes. The few grains in this lower half of the stratum corneum appeared to be predominantly over the intercellular domain (Fig. 1 H). The same silver grain distribution and localization was seen with EM autoradiography (Fig. 1 I).

Autoradiographs developed with GEA displayed slightly smaller silver grains than after D19b development when viewed with RCM (Fig. 1 J,K). Even at lower magnifications, these silver grains were still easy to detect (Fig. 1 J, non-coated slide). Sections thinner than 100 nm resulted in differently colored sections. However, longer autoradiography exposure times were necessary to obtain comparable grain densities, while the resolution appeared the same (Fig. 1 K, collodion coated slide, 75 nm section). While with LM autoradiography GEA-developed silver grains were easy detectable, in EM autoradiography the silver grains were hardly visible at low magnifications (Fig. 1 L). However, both distribution and localization of silver grains were identical. The small silver grain clusters appeared as single spots in the RCM.

DISCUSSION

The presented technique, a combination of high-resolution autoradiography and reflection contrast microscopy, allowed a sensitive and precise localization of silver grains over ultrathin sections of human stratum corneum. The use of exactly the same autoradiographical procedure for both the LM and EM level, i.e., ultrathin sections on collodion-coated glass slides covered with an emulsion monolayer, required only a change of the supporting medium (from slide to grid) to switch from light to electron microscopical visualization. Correlative studies with LM and EM autoradiography showed that the silver grain localization was identical at both levels.

Although the term "high-resolution autoradiography" usually refers to EM autoradiography (Salpeter, 1981), the technique presented here is a high-resolution detection of ^{3}H-E2 at the LM level. Resolution in autoradiography is usually expressed in half radius (HR) or half distance (HD) values, which is the distance from a radioactive point source (HR) or line source (HD) within half of the developed silver grains will be formed (Salpeter et al., 1969). HR and HD differ by a factor 1.7 ($HR = 1.7 \times HD$). For EM autoradiography, using 100 nm sections, an Ilford L4 monolayer, and Kodak D19b development, the experimentally determined HD, using a 50-nm-thick ^{3}H-labeled line source, was 187 nm (or HR of 318 nm; Kopriwa et al., 1984). The best spatial resolution for a light microscope fitted with an objective of numerical aperture 1.32 (as was used by us) is around 250 nm. Therefore, high-resolution LM autoradiography and high-resolution EM autoradiography with D19b development, as performed in this paper, have about the same autoradiographical resolution. We also used the fine grain developer GEA, which is known for its better resolution (HR of 196 nm/HD of 115 nm, Ginsel et al., 1979). In this case, the resolution of the proposed LM autoradiography technique is restricted by the quality of the optics of the light microscope.

The silver deposits after GEA development were often located in clusters. It is assumed that clustered silver deposits are derived from several latent images in a single exposed silver bromide crystal and, therefore, they are considered as one silver grain (Kopriwa, 1975; Vrensen, 1970). In fact, due to the limited resolution in light microscopy, these clusters were seen as single spots.

The application of high-resolution EM autoradiography in skin localization studies is rather rare (de Haan et al., 1989; Squier and Lesch, 1988). Based on the

Fig. 1. Autoradiographs of freeze-dried human stratum corneum after application of a ^{3}HE2 patch (A–C, F–L) or E2 patch (D,E) for 8 hours. The patch was removed before freeze-drying. A–C: Semithin sections, exposure time 30 days, Kodak D19b development. **A:** BFM image. **B:** RCM image of the same section, toluidine blue stained; **C:** RCM image, unstained section. D–I: Ultrathin sections, all Kodak D19b development, exposure times 30 days (D,G) and 103 days (E,F,H,I); **D:** RCM image, toluidine blue stained; **E:** RCM image, unstained, collodion coated slide; **F:** RCM image, unstained; **G:** RCM image, toluidine blue stained; **H:** RCM image, unstained, collodion coated slide; **I:** EM image. J–L: Ultrathin sections, all GEA development, exposure times 243 days (J) and 342 days (K, L); **J,K:** RCM image, unstained; **L:** EM image. sc = stratum corneum, ve = viable epidermis. Magnifications: For I and L see bar in I, for J see bar in J, all others see bar in A.

highest resolutions described in EM autoradiography literature, de Haan et al. (1989) concluded that the technique would make it possible to discriminate between inter- and transcellular drug transport across stratum corneum. High-resolution LM autoradiography will suffice too, considering that corneocytes are about 400–600 nm thick, the intercellular domain is about 100–140 nm wide, and the HD value for a 25-nm-thick radioactive line source is 196 nm (Ginsel et al., 1979). If ^{3}H-E2 diffuses via the intercellular domain, one can consider this domain as a radioactive line source with a width of 100–140 nm. Because this is thicker than 25 nm, the HD value will even be smaller than 196 nm. Then the resolution of the proposed LM autoradiography technique theoretically is sufficient to distinguish between inter- and intracellular localized silver grains in human stratum corneum. The observation that silver grains in the lower parts of the stratum corneum predominantly were located over or next to the intercellular domain could indicate that the intercellular domain is the predominant penetration route for ^{3}H-E2. However, it is also possible that the drug merely accumulated in the intercellular domains due to high local solubility. Time-dependent and pulse-chase permeation experiments could help to solve this problem.

Only recently, the use of confocal laser scanning microscopy was introduced in LM autoradiography (Watanabe et al., 1995a) and applied to skin distribution studies as well (Watanabe et al., 1995b). Confocal reflectance imaging, like DFM and EPM, gives dark-field images. In confocal transmission mode, it provides an image of the tissue. The main advantage of confocal laser scanning is that by optical sectioning of a thick photographic emulsion layer and subsequent overlapping of all these images including the confocal transmission image, a composition image can be obtained with all grains and tissue in focus (Watanabe et al., 1995a,b). For high-resolution LM autoradiography, which is performed with emulsion monolayers, this advantage does not apply.

In conclusion, RCM visualization of autoradiographs derived from unstained ultrathin sections combines the benefits of LM and EM autoradiography. Several different sections can be placed on a single slide and, therefore, processed for autoradiography in exactly the same manner. RCM allows a fast and easy examination of large section areas at low magnifications while both tissue and silver grains are visible. At high magnification, ^{3}H-E2 was successfully localized in human stratum corneum with an autoradiographical resolution similar to EM autoradiography.

ACKNOWLEDGMENTS

The author thanks Frans Prins for providing the reflection contrast microscope, and Ger Renes, for putting the electron microscope at my disposal.

REFERENCES

Bidmon H-J, Pitts JD, Solomon HF, Bondi JV, Stumpf WE. 1990. Estradiol distribution and penetration in rat skin after topical application, studied by high resolution autoradiography. Histochemistry 95:43–54.

Conte L, Ramis J, Mis R, Forn J, Vilaró S, Reina M, Vilageliu J, Basi N. 1992. Percutaneous absorption and skin distribution of [^{14}C]flutrimazole in mini-pigs, Arzneim-Forsch/Drug Res 42:847–853.

Cornelese-ten Velde I, Prins FA. 1990. New sensitive light microscopical detection of colloidal gold on ultrathin sections by reflection contrast microscopy. Histochemistry 94:61–71.

Cornelese-ten Velde I, Bonnet J, Tanke HJ, Ploem JS. 1990. Reflection contrast microscopy performed on epi-illumination microscope stands; comparison of reflection contrast- and epi-polarization microscopy. J Microsc 159:1–13.

de Haan FHN, Boddé HE, de Bruin WC, Ginsel LA, Junginger HE. 1989. Visualizing drug transport across stratum corneum: cryotechniques, vapour fixation, autoradiography. Int J Pharm 56:75–86.

de Mey J. 1983. Colloidal gold probes in immunohistochemistry. In: Polak JM, van Noorden S, editors. Immunohistochemistry. Practical applications in pathology and biology. Bristol, UK: J Wright and Sons. p 82–112.

Ginsel LA, Onderwater JJM, Daems WT. 1979. Resolution of a gold latensification-elon ascorbic acid developer for Ilford L4 emulsion. Histochemistry 61:343–346.

Hoefsmit ECM, Korn C, Blijleven N, Ploem JS. 1986. Light microscopical detection of single 5 and 20 nm gold particles used for immunolabelling of plasma membrane antigens with silver enhancement and reflection contrast. J Microsc 143:161–169.

Kopriwa BM. 1975. A comparison of various procedures for fine grain development in electron microscopic radioautography. Histochemistry 44:201–224.

Kopriwa BM, Levine GM, Nadler NJ. 1984. Assessment of resolution by half distance values for tritium and radioiodine in electron microscopic radioautographs using Ilford L4 emulsion developed by "Solution Physical" or D-19b methods. Histochemistry 80:519–522.

Krum JM, Rosenstein JM, Silverman WF. 1991. An alternate method for staining plastic embedded autoradiographs. J Histotechnol 14:43–45.

Neelissen JAM, de Haan FHN, Schrijvers AHGJ, Junginger HE, Boddé HE. 1996. Optimization and validation of freeze-drying for light and electron microscopic autoradiography of percutaneous steroid transport. J Control Rel 42:1–13.

Neelissen JAM, Arth C, Schrijvers AHGJ, Junginger HE, Boddé HE. 1998. Validation of freeze-drying to visualize percutaneous ^{3}H-estradiol transport: the influence of skin hydration on the efficacy of the method. Skin Pharmacol Appl Skin Physiol 11:11–22.

Ploem JS. 1975. Reflection-contrast microscopy as a tool for investigation of the attachment of living cells to a glass surface. In: van Furth R, editor. Mononuclear phagocytes in immunity, infection and pathology. Oxford: Blackwell. p 405–421.

Priestley JV. 1992. Epi-polarised illumination and emulsion autoradiograms. Eur Microsc Anal Nov:17–19.

Prins FA, van Diemen-Steenvoorde R, Bonnet J, Cornelese-ten Velde I. 1993. Reflection contrast microscopy of ultrathin sections in immunocytochemical localization studies: a versatile technique bridging electron microscopy with light microscopy Histochemistry 99:417–425.

Rapaport DH, Herman KG; MM LaVail. 1992. Epi-polarization and incident light microscopy readily resolve an autoradiographic or heavy metal label from an obscuring background or second label. J Neurosci Methods 41:231–238.

Rogers AW. 1967. Techniques of autoradiography, Amsterdam: Elsevier..

Rutherford T; Black JG. 1969. The use of autoradiography to study the localization of germicides in skin. Br J Dermatol 81 Suppl 4:75–87.

Salpeter MM. 1981. High resolution autoradiography. In: Techniques in the life sciences. Techniques in cellular physiology. Shannon, Ireland: Elsevier. p P106/1–45.

Salpeter MM, Bachmann L, Salpeter EE. 1969. Resolution in electron microscope radioautography. J Cell Biol 41:1–20.

Singh RN. 1986. How to increase the effective depth of focus of the light microscope for photography. Stain Technol 61:17–20.

Squier CA, Lesch CA. 1988. Penetration pathways of different compounds through epidermis and oral epithelia. J Oral Pathol 17:512–516.

Suzuki M, Asaba K, Komatsu H, Mochizuka M. 1978. Autoradiographic study on percutaneous absorption of several oils useful for cosmetics. J Soc Cosmet Chem 29:265–282.

Touitou E, Fabin B, Dany S, Almog S. 1988. Transdermal delivery of tetrahydrocannabinol. Int J Pharm 43:9–15.

Vrensen GFJM. 1970. Some new aspects of efficiency of electron microscopic autoradiography with tritium. J Histochem Cytochem 18:278–290.

Watanabe M, Koide T, Konishi M, Kanbara K, Shimada M. 1995a. Use of confocal laser scanning microscopy in radioautographic study. Cell Mol Biol 41:131–136.

Watanabe H, Watanabe M, Jo N, Kiyokane K, Shimada M. 1995b. Distribution of [1,2-^{3}H]taurine in the skin of adult and newborn mice studied by microautoradiography. Cell Mol Biol 41:49–55.

Zelei BV, Walker CJ, Sawada GA, Kawabe TT, Knight KA, Buhl AE, Johnson GA, Diani AR. 1990. Immunohistochemical and autoradiographic findings suggest that minoxidil is not localized in specific cells of vibrissa, pelage, or scalp follicles. Cell Tissue Res 262:407–413.